The Application of an Active Power Filter on a Photovoltaic Power Generation System

Bouzelata Yahia*, Djeghloud Hind**‡, Chenni Rachid**

* University Mentouri of Constantine, MoDERNa Laboratory

** University Mentouri of Constantine, Laboratory of Electrical Engineering of Constantine 'LGEC'

yahia_elt1@yahoo.fr, hinddjeghloud@yahoo.fr, rachid.chenni@gmx.fr

‡ Corresponding Author; Djeghloud Hind, University Mentouri of Constantine, Laboratory of Electrical Engineering of Constantine 'LGEC', Constantine 25000, Algeria, 213-31819013, hinddjeghloud@yahoo.fr

Received: 08.07.2012 Accepted: 17.08.2012

Abstract- This paper deals with the Photovoltaic (PV) power generation system (PVGS) associated with active power filtering (APF) operation. PVGS is a promising source of energy with great interest in clean and renewable energy sources. The rising number of power electronics-based equipment is resulting in quality problems of electric power supply. Both high power industrial loads and domestic loads cause many disturbances in the utility side such as harmonics, imbalance, sags, swells, flickers and frequency variation. Power quality problems may arise in the system or may be created by the consumer itself. The proposed PVGS associated with an APF is able not only to track the maximum power point of the photovoltaic energy but also to dampen harmonic currents from the grid line. To achieve these purposes, first the output voltage of PV generator is increased using a simple power electronic interface connected to PV array based on a boost converter. The controller extracts maximum power from the solar array. A closed loop scheme employing a PI controller has been modeled to regulate the DC-bus voltage feeding the converter. Secondly, a study of a PV system combined with the function of the active power filtering system is provided and which permits the cancellation of the most noteworthy harmonics from the utility current. The APF system is based on a two-level voltage source inverter adopting P-Q theory algorithm for references harmonic currents extraction. To demonstrate the performance of abovementioned PVGS with APF, a MATLAB/Simulink model has been established and simulated. Results seem to be very promising.

Keywords- Photovoltaic power generation system PVGS; maximum power point tracker MPPT, boost chopper, harmonic disturbance, nonlinear load, active power filtering APF.

1. Introduction

Photovoltaic energy system is one of the cleanest power generating technologies available today with very little impact on the environment. When PV operates, it converts the sun's rays into electricity, producing no air pollution, waste, or noise.

The more use of PV energy to generate electricity from the sun rays decreases our dependence on fossil fuels and on imported sources of energy. As a result, solar energy can be an effective economic development driver. The world PV market installations reached a record higher to 7.3 gigawatts (GW) in 2009, representing a growth of 20% over the previous year [1].

On the other hand, with significant development of power electronics technology, the proliferation of nonlinear loads such as static power converters has deteriorated power quality in power transmission/distribution systems Notably, In order to compensate harmonics in power transmission/distribution systems, active filters (AF) have been speedily expanding with power electronics technology. Since their basic compensation principles were proposed around 1970, much research has been done on active filters and their practical applications [2-4].

The main purpose of the active filters installed by individual consumers is to compensate for current harmonics and/or current imbalance of their own harmonic-producing loads.

In this paper, PV-AF system using the P-Q theory method for APF to compensate the undesired components of unbalanced loads and fast tracking of MPP in PV array confirmed that it is possible to combine the AF theory to the three phase PV system connected to the utility in order to improve the power quality.

The paper is organized as follows; PV-AF system control scheme is analyzed in Section 2 in three point, Photovoltaic power generation system, and Shunt active filter and PV-AF system, next, the simulation results are discussed in Section 3. Finally, the conclusion is presented in Section 4.

2. PV-AF System Control Scheme

2.1. Photovoltaic Power Generation System

Photovoltaic (PV) is a rapidly developing electricity generation technology, two types of PV cell application can be distinguished: stand-alone and grid-connected [5-7].

In stand-alone application the PV system functions independently of the electricity network. For example, we can cite energy supply for water pumping systems. In the case of a grid-connected system, there is an exchange of energy between the PV system and the grid.

A current source anti-parallel with a diode is the simplest representation of electrical equivalent circuit for a solar cell. The Kirchhoff's law gives [8]:

$$I = I_{pv} - I_0\left(e^{\left(\frac{q(V+R_sI)}{\alpha KT}\right)} - 1\right) - \frac{V + R_sI}{R_{sh}} \quad (1)$$

Where, I_{pv} is photocurrent; I_0 is diode saturation current; q is Coulomb constant (1.602×10^{-19}C); K *is* Boltzmann's constant (1.381×10^{-23} J/K); T is cell temperature in °K; α is P-N junction ideality factor; R_s and R_{sh} are the intrinsic series and shunt resistances of the cell, respectively.

As the photovoltaic power varies with the climatic conditions, there is no explicit reference power for tuning. The PV voltage needs to be adjusted according to the solar radiation to extract the maximum photovoltaic current.

2.1.1. MPPT Control

To obtain the maximum power from PV array, the best choice of MPPT technique is extremely important. The literature, for example ref. [9], shows that the Perturb and Observe 'P&O' technique has relatively good tracking performance. Therefore this technique was chosen as the MPPT algorithm for this study and was implemented in simulation by the block diagram shown in "Fig. 1". "Table 1" summarizes the settled 'P&O' algorithm result where the MPP is situated at 54.7V exactly, in this point *Pmax* is 315W. The developed Simulink model allowing the application of the algorithm of "Fig. 1" is portrayed in "Fig. 2" where the algorithm is incorporated in a MATLAB function. "Figure 3" illustrates how to obtain *Pmax*, *Vmax* and *Pmax* on the basis of the 'P & O' algorithm.

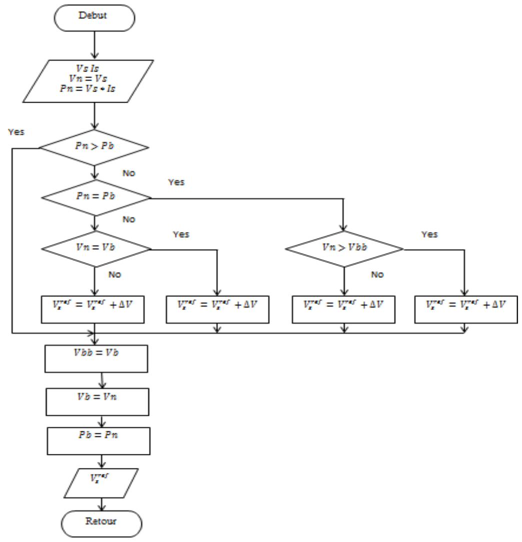

Fig. 1. Flowchart of the P&O MPPT method.

Table. 1. Determination of MPP

Vs(i)[V] i=1:66	**Vs(54)=53V**	**Vs(55)=54V**	**Vs(56)=55V**
V_s [V]	53.7	54.7	54.3
P_s [W]	313.51	315.05	314.84

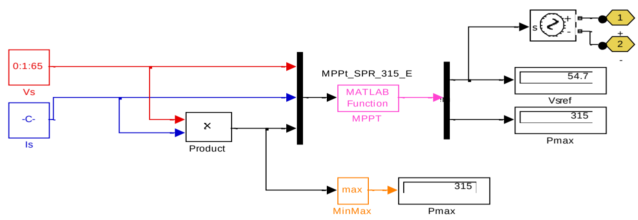

Fig. 2. Simulink model of the studied MPPT

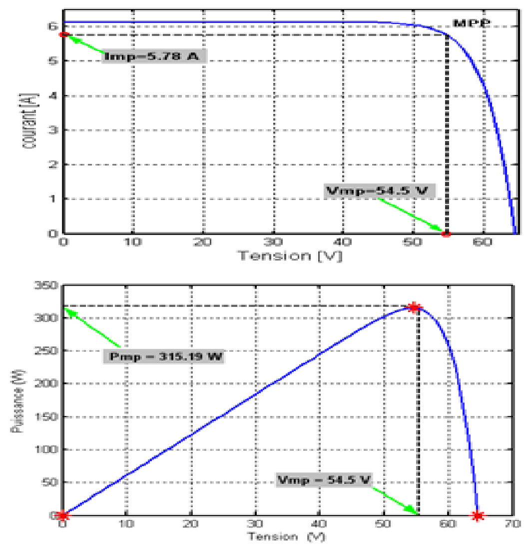

Fig. 3. Location of *Pmax*, *Vmax* and *Imax* in a PV array.

2.1.2. Increase and Regulation of the Output Voltage of PV Modules

To ensure the level of voltage needed to supply the power circuit of the APF (≈ 750 V), we put 4 modules in series of the proposed SPR-315 panel. With this composition, we could raise the voltage level of the PV system considered, from 54.7 V to 218.8 V, and then to arrive to 750 V, we inserted a boost converter.

Boost converter is a DC-DC converter that steps up its input voltage based on the formula given in "Eq. (2)" [10]:

$$V_{out} = \frac{1}{1-D} V_{in} \tag{2}$$

Where *Vout* is the output voltage of the boost converter, *Vin* is the input voltage and D is the duty cycle which is the ratio between the time within which the GTO. The circuit diagram of the boost converter combined with a PV generator is shown in "Fig. 4". It consists of an inductor, a GTO switch, a fast switching diode and a capacitor. When the GTO is switched ON, the inductor is directly connected to the input voltage source. In this case, the inductor current rises charging it and the inductor is storing energy while the diode is reverse biased disconnecting the load (R) and output capacitor (C) from the source voltage. In this case, the pre-charged capacitor assures constant voltage across the load terminals. When the GTO is switched OFF, the diode is forward biased and both the source and the charged inductor are connected to the load. The inductor releases the energy stored in it. This energy is transferred to the load in the form of voltage that adds to the source voltage. Hence, the converter has boosts the input voltage.

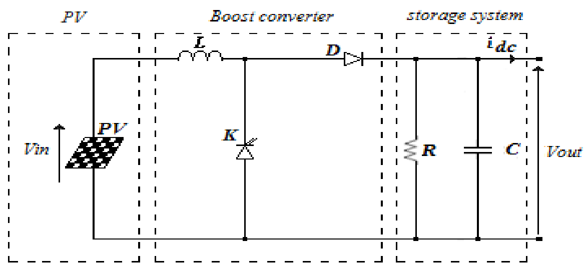

Fig. 4. Association PV generator and boost chopper

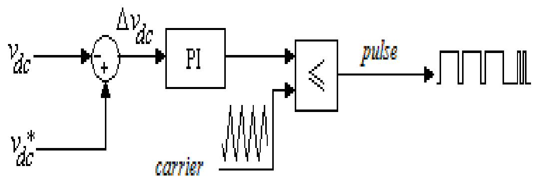

Fig. 5. Control loop of the DC-bus voltage

In order to regulate the DC-bus voltage (V_{out}) and to achieve the voltage level 750v required to supply the power circuit of AF, we designed the control loop shown in "Fig. 5".

First, V_{dc} is measured by a voltage sensor (voltage measurement), then compared to a reference $V_{dc}*$. After the error is corrected ΔV_{dc} using a PI controller. The output of the PI is then regarded as the modulating a PWM modulator intersective.

The design parameters of the PI controller are as follows:

The power P_{dc} is expressed depending on the voltage V_{dc}, by:

$$Pdc = \frac{d}{dt}\left(\frac{1}{2}.C.Vdc^2\right) \tag{3}$$

For small variations of V_{dc} around $V_{dc}*$, "equation (3)" becomes:

$$P_{dc} = V_{dc}^*.C.\frac{dV_{dc}}{dt} \tag{4}$$

$$\Rightarrow \quad V_{dc} = \int \frac{P_{dc}}{V_{dc}.C} dt \cong \frac{P_{dc}}{V_{dc}^*.C.p} \tag{5}$$

The principle of correction of the PI system is indicated in "Fig. 6".

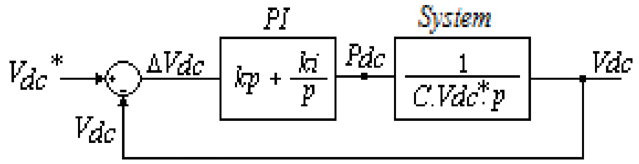

Fig. 6. Principle of regulation of *Vdc* by the use of a PI controller

So the transfer function is $TF = \frac{V_{dc}}{\Delta V_{dc}} = PI * système$

TF of the open loop (OLTF)

$$\Rightarrow \quad OLTF = \left[k_p + \frac{k_i}{p}\right].\frac{1}{C.V_{dc}^*.p} = \frac{p+\frac{k_i}{k_p}}{\frac{p}{k_p}}.\frac{\frac{1}{C.V_{dc}^*}}{p}$$

$$OLTF = \frac{p+\frac{k_i}{k_p}}{\frac{p}{k_p}}.\frac{\frac{1}{C.V_{dc}^*}}{p}$$

En posant $p + \frac{k_i}{k_p} = p \Rightarrow \boldsymbol{k_i = 0}$

$$\Rightarrow \quad OLTF = \frac{\boldsymbol{k_p}}{\boldsymbol{C.V_{dc}^*p}}$$

TF of the close loop (CLTF)

$$FTBF = \frac{FTBO}{1+FTBO} = \frac{\frac{k_p}{C.V_{dc}^*.p}}{1+\frac{k_p}{C.V_{dc}^*.p}} = \frac{1}{\frac{C.V_{dc}^*}{k_p}.p+1}$$

$$Où \ \tau = \frac{C.V_{dc}^*}{k_p} \quad \Rightarrow \quad \boldsymbol{k_p} = \frac{\boldsymbol{C.V_{dc}^*}}{\boldsymbol{\tau}}$$

Finally, "Figure 7" shows the established Simulink model of a PV system fed boost DC chopper. The simulation of this model is carried out using the parameters recorded in "Table 2". The simulation result is depicted in "Fig. 8" where we observe a perfect correspondence between the system DC output voltage and its reference (750V), the output voltage will serve to feed the inverter.

Table 2. Simulation parameters of the association PV generator and boost chopper

parameters	numerical values
V_m	218.8 V
R	300 Ω
C	1820 µF
L	0.5 mH
V_m*	750 V
τ	40
Switching frequency	2KHz
carrier amplitude	(85, -10)

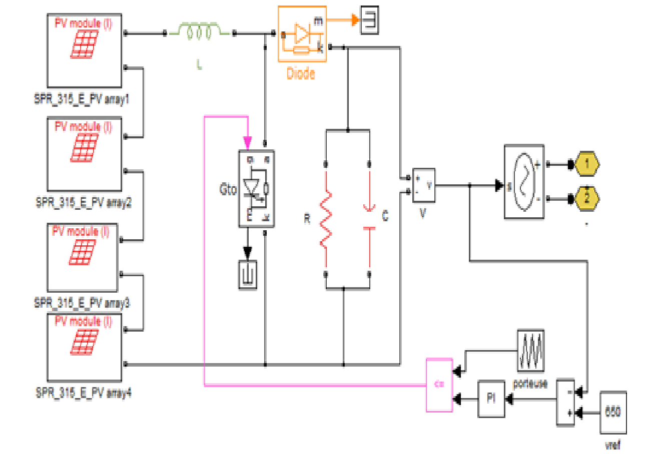

Fig. 7. Simulink model of all PV-Boost chopper with a storage system

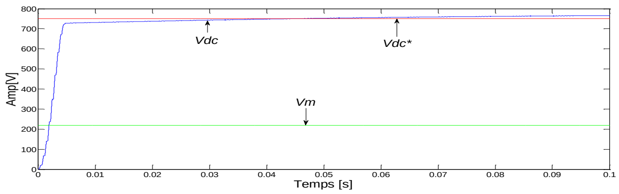

Fig. 8. Output voltage of the boost chopper (V_{dc})

2.2. Shunt Active Filter

APF is a power electronic device used to suppress harmonic and compensate reactive power dynamically, which can compensate harmonic and reactive current that both of the frequency and amplitude are varying, overcoming deficiencies of traditional harmonic suppression and reactive power compensation way of Reactive Power Filter. "Figure 9" displays a basic shunt active power filter block diagram.

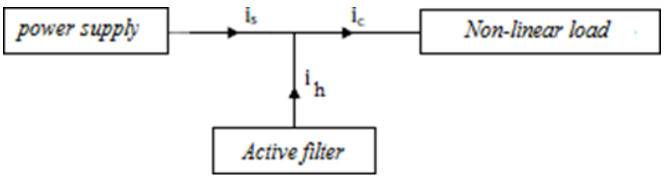

Fig. 9. Block diagram of shunt active power filter.

The general structure of the shunt active filter is in the form of two blocks, the power part and the control part. The power section consists [11]:

1. Voltage inverter: it comprises three arms reversible switches to current, made up from a transistor (IGBT or GTO) and a antiparallel diode,

2. Energy storage system: the energy storage on the DC side often signified by a capacitive storage system represented by a capacitor Cdc which acts as a DC voltage source V_{dc}.

3. The output filter: is a passive filter used to connect the voltage inverter to the grid and to absorb high frequency harmonics due the cuttings caused by the pulse generator.

The control part consists of:

1. The method of identifying current disturbed: there are mainly two kinds of control strategies for extracting current or voltage harmonics from the corresponding distorted current or voltage harmonics. One is based on the *Fourier* analysis in frequency domain [12], and the other is based on the theory of instantaneous reactive power in three-phase circuits which is called the "P-Q theory" proposed by Hirofumi Akagi [7].

2. Regulating the DC voltage: the average voltage V_{dc} across the capacitor must be maintained at a fixed value. The main causes of change are losses in the active filter (switches and output filter) [11].

3. The control of the inverter: the aim of the inverter control is to allow the best reproduction of disturbed currents of reference through the control commands applied to the power switches. The two main families the control of static converters are:

- hysteresis control,
- Pulse-width-modulation control.

The concept of the "P-Q theory" in the time-domain has been applied to the control strategy of almost all the active filters by individual high power consumers. The general *dq* transformation is used in this paper to compensate the negative component and the harmonics component. Using *dq* transformation as described in "Eq. (6)" [7],

$$\begin{bmatrix} v_\alpha \\ v_\beta \end{bmatrix} = [C_{32}].\begin{bmatrix} v_a \\ v_b \\ v_c \end{bmatrix}, \quad \begin{bmatrix} i_\alpha \\ i_\beta \end{bmatrix} = [C_{32}].\begin{bmatrix} i_a \\ i_b \\ i_c \end{bmatrix} \tag{6}$$

C_{32}: the transformation matrix developed by Concordia is given by:

$$[C_{32}] = \sqrt{\frac{2}{3}}.\begin{bmatrix} 1 & -1/2 & -1/2 \\ 0 & \sqrt{3}/2 & -\sqrt{3}/2 \end{bmatrix} \tag{7}$$

This transformation is valid only if the sum: *va(t)+vb(t)+vc(t)* equals zero, and if the voltages are balanced and sinusoidal. The instantaneous active and reactive powers in this frame are calculated by:

$$p(t) = v_\alpha(t).i_\alpha(t) + v_\beta(t).i_\beta(t) \tag{8}$$

$$q(t) = -v_\alpha(t).i_\beta(t) + v_\beta(t).i_\alpha(t) \tag{9}$$

It is obvious that *p(t)* is identical to its conventional expression in the a-b-c reference. However, to define the instantaneous reactive power, Akagi introduced a new term in the vector space given by:

$$\vec{q} = \vec{v}_\alpha \times \vec{i}_\beta + \vec{v}_\beta \times \vec{i}_\alpha \tag{10}$$

From "Eq. (8)" and "Eq. (9)", *p* and *q* can be expressed in AC and DC components, such as:

$$p = \bar{p} + \tilde{p} \tag{11}$$

$$q = \bar{q} + \tilde{q} \tag{12}$$

$\bar{p}$: DC Component of *p* related conventional fundamental active current

$\tilde{p}$: AC component of *p*, free of mean value and related to the harmonic currents caused by the AC components of the real instantaneous power

$\bar{q}$: DC component of *q* related to the reactive power generated by the fundamental components of currents and voltages

$\tilde{q}$: AC component of *q* and related harmonic currents caused by the AC component of instantaneous reactive power

The expression of the currents as a function of instantaneous power in the plane α-β is given by:

$$\begin{bmatrix} i_\alpha \\ i_\beta \end{bmatrix} = \frac{1}{v_\alpha^2 + v_\beta^2} \cdot \left\{ \begin{bmatrix} v_\alpha & v_\beta \\ v_\beta & -v_\alpha \end{bmatrix} \cdot \begin{bmatrix} p \\ 0 \end{bmatrix} + \begin{bmatrix} v_\alpha & v_\beta \\ v_\beta & -v_\alpha \end{bmatrix} \cdot \begin{bmatrix} 0 \\ q \end{bmatrix} \right\} = \begin{bmatrix} i_{\alpha p} \\ i_{\beta p} \end{bmatrix} + \begin{bmatrix} i_{\alpha q} \\ i_{\beta q} \end{bmatrix} \tag{13}$$

Now if you want also compensate the reactive power (displacement power factor), and the harmonic currents generated by nonlinear loads, the reference signal of the parallel active filter must include $\tilde{p}$, $\bar{q}$ and $\tilde{q}$. In this case, the reference currents are calculated by:

$$\begin{bmatrix} i_\alpha^* \\ i_\beta^* \end{bmatrix} = \frac{1}{v_\alpha^2 + v_\beta^2} \cdot \begin{bmatrix} v_\alpha & v_\beta \\ v_\beta & -v_\alpha \end{bmatrix} \cdot \begin{bmatrix} \tilde{p} \\ \bar{q} + \tilde{q} \end{bmatrix} \tag{14}$$

The final compensation currents in the *a-b-c* reference, including the zero sequence components, are given by:

$$\begin{bmatrix} i_a^* \\ i_b^* \\ i_c^* \end{bmatrix} = \sqrt{\frac{2}{3}} \cdot \begin{bmatrix} 1/\sqrt{2} & 1 & 0 \\ 1/\sqrt{2} & -1/2 & \sqrt{3}/2 \\ 1/\sqrt{2} & -1/2 & -\sqrt{3}/2 \end{bmatrix} \cdot \begin{bmatrix} -i_0 \\ i_\alpha^* \\ i_\beta^* \end{bmatrix} \tag{15}$$

$$i_0 = \frac{1}{\sqrt{3}} \cdot (i_a + i_b + i_c) \tag{16}$$

The block diagram for generating the reference currents of the "Eq. (15)" is shown in "Fig. 10",

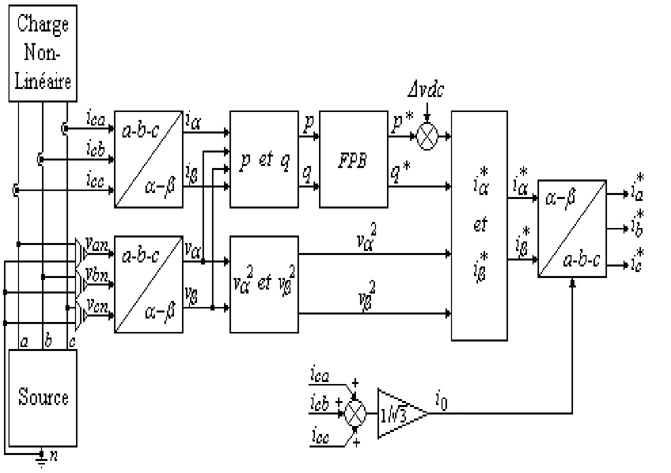

Fig. 10. Block diagram for generating reference currents according to the *p-q* theory.

2.3. AF System Supplied by DC Source

The active power filter supplied by DC source is show in the "Fig.11"

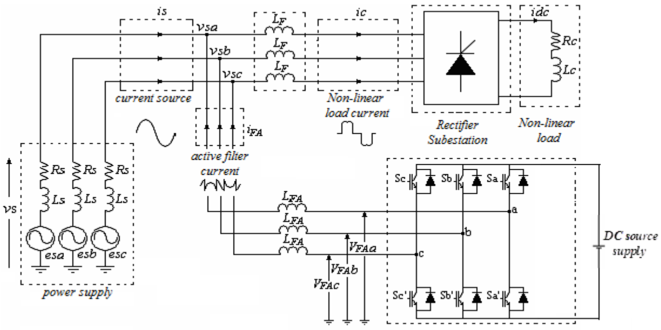

Fig. 11. Circuit diagram of the AF system supplied by DC source.

2.4. PV-AF System

Photovoltaic (PV) grid-connected power conditioning systems have attracted considerable attention worldwide due to their potential dual functions [13-14]: they can feed the active power from PV arrays into the utility network; and they can improve power quality through elimination of unwanted harmonics and compensation of the reactive power requirements of nonlinear loads.

PV-AF system's basic hardware composition is similar to that of general PV power generation systems. The AF system's compensation theory is applied to the inverter control algorithm. Including the AF function from the PV power generation system connected to the utility would help to improve power quality [15]. The main circuit diagram of the PV-AF system proposed in this work is shown in "Fig. 12". In this system, constant voltage control for MPPT is applied [16]. The PV-AF system has two kinds of current references, one to control PV output power (MPPT control, constant voltage control, etc.) [16], [17], and another for the AF function. The latter detects the load's harmonic currents and compensates with the same amount of detected harmonic currents for the utility grid. Because the target of the proposed PV-AF system is that the conventional PV system also plays the AF system role, the fundamental circuit of hardware is almost the same as the conventional three-phase PV system connected to the utility [18], [19].

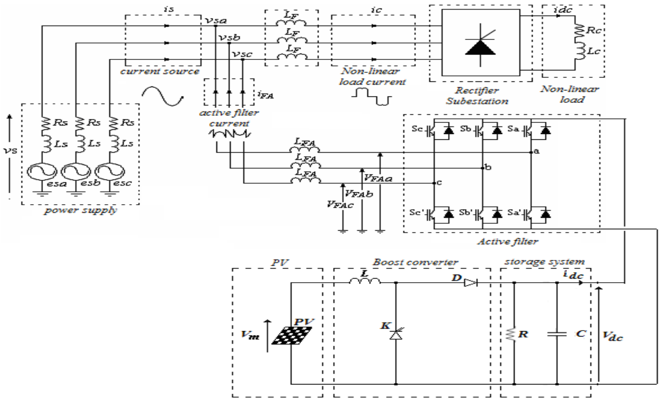

Fig. 12. Circuit diagram of the PV-AF system.

3. Simulation Results and Discussion

For verification, simulating investigations of the proposed system are performed using Matlab/Simulink software under the conditions reported in “Table 3”. In this section simulation results are given for two functional operations before compensation and after compensation.

Table 3. Simulation parameters

parameters	numerical values
Power supply	
rms voltage	230 V
frequency f	50Hz
Line impedance (*Rs,Ls)*	(0.5 mΩ, 19 μH)
Loads to protect	
Load resistance DC *Rc*	6Ω,
Load inductance DC *Lc*	20mH
Parallel active filter	
(Lf)	1 mH,
Switching frequency	10 kHz.
Continuous common source	
Vdc	750 V
Control	
Carrier frequency	10 kHz
Carrier amplitude	20

3.1. Results Before Compensation

Graphs of the source current before application of active filtering are shown in “Fig. 13”, “Fig. 14” and “Fig. 15”. There is a symmetrical current *isa* distortion from the point of half period “Fig.14”, confirmed by the spectrum *isa*. “Figure 15” representing the top 25 most significant harmonics, with a THDi of 25.58% for an observation period of 0.1 s, was recorded also degradation in power factor (cosφ=0.8).

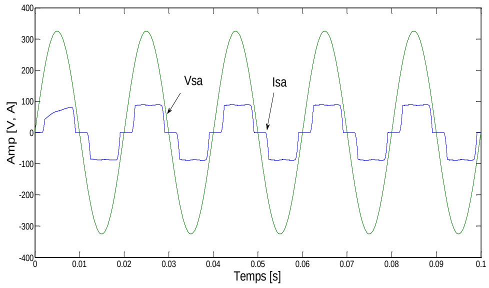

Fig. 13. Source current and voltage for uncompensated distribution system of phase-a.

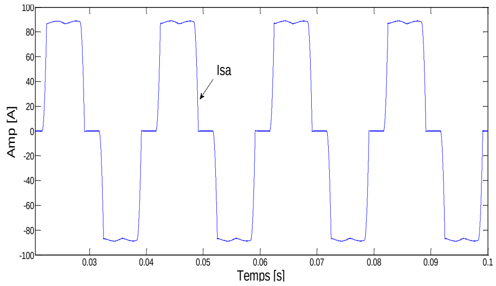

Fig. 14. Source current for uncompensated distribution system of phase-a.

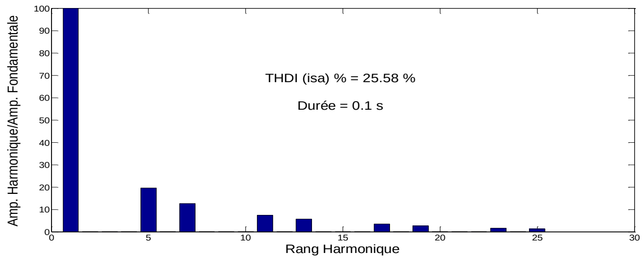

Fig. 15. Harmonic spectrum of source current before compensation.

3.2. Results After Compensation

A. AF System Supplied by DC Source

After application of the active filter supplied by DC source, there was a marked improvement in the shape of *isa*, as shown in “Fig.16”, Improvement in the harmonic spectrum “Fig.17”, with a THDi of 1.90% for 0.1 s and improvement of (*cosφ=0.969*).

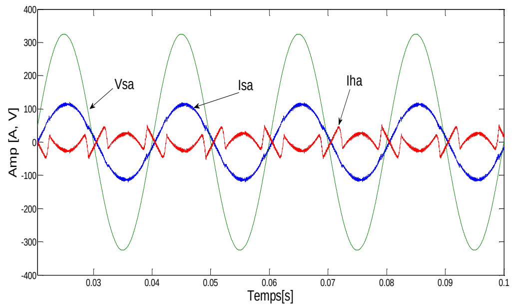

Fig. 15. Source current, voltage and harmonic current for compensated distribution system of phase-a.

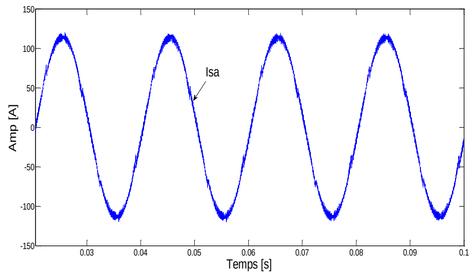

Fig. 16. Source current for compensated distribution system of phase-a.

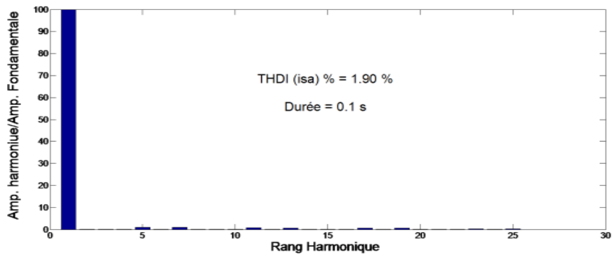

Fig. 17. Harmonic spectrum of source current after compensation.

B. PV-AF System

After application of the active filter, there was a marked improvement in the shape of isa, as shown in “Fig.19”. The harmonic spectrum of “Fig.20”, confirmed that isa has been cleared at a fairly suitable, with a THDi of 1.91% for 0.1 s. Moreover, there is an improvement of ($cos\varphi = 0.97$).where *isa* and *vsa* are in phase “Fig.18”. The active filter generated a harmonic current iha shown in “Fig.18” reflecting that *isa* has recovered its sinusoidal shape.

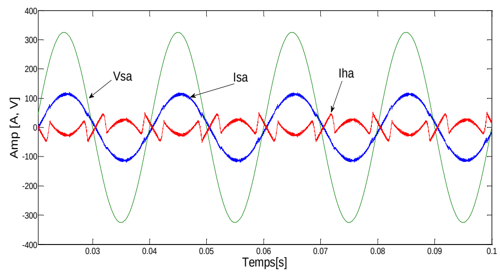

Fig. 18. Source current, voltage and harmonic current for compensated distribution system of phase-a.

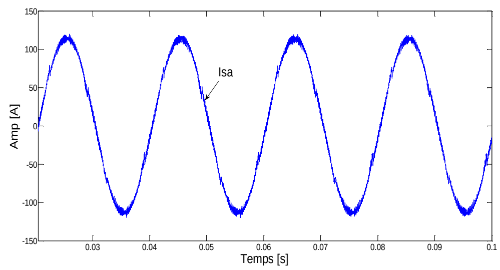

Fig. 19. Source current for compensated distribution system of phase-a.

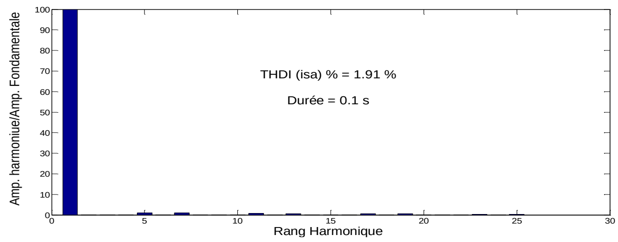

Fig. 20. Harmonic spectrum of source current after compensation.

3.3. Comparison

We observe a small deference in the improvement of the harmonic spectrum “Fig.17” when THDi = 1.90% in the case of AF system supplied by DC source, “Fig. 20” when THDi = 1.91% in the case of PV-AF system.

4. Conclusion

In this paper, the PV-AF system is proposed and confirmed that it is possible to combine APF theory to the three phase PV system connected up to utility. Using simulation analysis, it is theoretically positive to actualize the PV-APF system using instantaneous power theory which is found to be an effective solution for improving power quality. The proposed topology reduces harmonics and provides reactive power compensation due to non-linear load current. As a result source current become sinusoidal and unity power factor is also achieved. As evident from the simulation studies that photovoltaic based shunt active filter is effective for power conditioning applications. The THD of the source current after compensation is 1.91 % “Fig. 20” which is less than 5 % required by the IEEE-519 standards limiting the total harmonic distortion in distribution networks.

The proposed study presented in this paper is being pursued within the framework of a PhD thesis, where the prospects are firstly the practical application of the theoretical works, then a hybrid connection of the PVGS with a wind generation system, the whole are to be grid connected after that. The power quality concerns will be considered as well.

References

[1] “Solar Market Research and Analysis”, http://www.solarbuzz.com.

[2] L. Gyugyi & C. Strycula, “active AC Power Filters”, IEEENRS '76 Annual Meeting, pp. 529 (1976).

[3] H. Akagi, Y. Kanmwva, K. Fujiia, A. Nabae, “Generalized Theory of the instantaneous Reactive Power and its Application”, Trans. IEE Jopon.Vol. 103-H, No. 7. 1983, pp.4148.

[4] L. Gyugi, “Unified Power-Flow Control Concept for Flexible AC Transmission Sync motor”. IEE ~Proceeding -C, Vol. 139, pp. 323-33 I, July 1992.

[5] M. A. Slonim and L. M. Rahovich, “Maximum power point regulator for 4 kW solar cell array connected through invertor to the AC grid,” in Proc. 31st Intersociety Energy Conver. Eng. Conf., 1996, pp. 1669-1672.

[6] J. Harada and G. Zhao, “Controlled power-interface between solar cells and ac sources,” in IEEE Telecommun. Power Conf., 1989, pp. 22.1/1-22.1/7.

[7] H. Ryong Seo, G. Hun Kim, M. Ali, M. Park, I. keun Yu, “A study on the Performance Analysis of the Grid-Connected PV-AF System,” in Proc. International Conference on Electrical Machines and Systems 2007 pp. 641-773.

[8] R. Gupta, A. Ghosh and A. Joshi, “Cascaded multilevel control of DSTATCOM using multiband hysteresis modulation”, IEEE Power Eng. Soc. General Meeting, pp.18-22, Jun. 2006.

[9] F. R. Islam, H. R. Pota, “Design a PV-AF system using V2G Technology to Improve Power Quality” IECON 2011, pp. 861 - 866 , 7-10 Nov. 2011.

[10] M. Elshaer, A. Mohamed, and O. Mohammed, “Smart Optimal Control of DC-DC Boost Converter in PV Systems” IEEE Transmission and Distribution Conference and Exposition Latin America, 2010, pp. 978-1-4577-0487-1/10.

[11] M.A.E. Allali, “Contribution à l’étude des compensateurs actifs des réseaux électriques basse tension”, PhD Thesis, ULP Strasbourg I. 12, Sept 2002.

[12] W. M. Grady, M. J. Samotyj, and A. H. Noyola, "Survey of Active Power Line Conditioning Methodologies," IEEE Trans. Power Delivery, Vol. 5, pp. 1536-1542, 1990.

[13] S. B. Kjaer, J. K. Pedersen, F. Blaabjerg. "A Review of Single-Phase Grid-Connected Inverters for Photovoltaic Modules", IEEE Transactions on Industry Applications, vol. 41, no. 5, Sept/Oct. 2005, pp. 1292-1306.

[14] P. C. Loh, D. M. Vilathgamuwa, C. 1. Gajanayake, Y.R. Lim and C.W. Teo. "Transient Modeling and Analysis of Pulse-Width Modulated Z Source Inverter", IEEE Transactions on Power Electronics, vol. 22, no. 2, Mar. 2005, pp.498-507.

[15] Gyeong-Hun Kim, Hyo-Rong Seo, Minwon Park, Mohd. Hasan Ali, In-keun Yu, Jin-Hong Jeon, Seul-Ki Kim, and Jong-Bo Ahn, “A Novel Anti-islanding method in the three phase PV-AF power generation system,” IASTED2008, Langkawi, April 2008.

[16] J. Chou, Y. Makino, Y. Hukuda, A. Danaka, and E. Taniguchi, “A Study on the Constant Voltage Control of Photovoltaic Generation,” National Convention Record IEEJ, Vol. 588, No.5, pp.161-162, 1993.

[17] T. Kawamura, K. Harada, Y. Ishihara, T. Todaka, T. Oshiro, H. Nakamura, M. Imataki, “Analysis of MPPT Characteristics in Photovoltaic Power System”, Journal, Solar Energy Materials and Solar Cells, Vol.47, pp.155-165, 1997.

[18] Y.G. Park, M. Park and I.K. Yu, “A Study on the Utility Interactive PV Power Generation System Adding the Function of Shunt Active Filter,” ICEE 2005, China, July, 2005.

[19] M. Park, N.G. Seong and I.K. Yu, “A Novel Photovoltaic Power Generation System including the Function of Shunt Active Filter,” KIEE International Transactions on EMECS, Vol. 3B-2, pp. 103- 110, June, 2003.